Scilight

Advanced Antibacterial Materials

https://www.sciltp.com/journals/aam

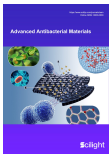

Article

Bacteria-Identifiable 2D Violet Phosphorene-Based Nanosystems for Sepsis Diagnosis and Blood Disinfection

Qiudi Shen [1], Zhihao Li [2], Xuewen Zhao [3], Jing Kang [1,*], Jinying Zhang [3,*] and Alideertu Dong [1,*]

[1] College of Chemistry and Chemical Engineering, Engineering Research Center of Dairy Quality and Safety Control Technology, Ministry of Education, Inner Mongolia University, 235 University West Street, Hohhot 010021, China
[2] Department of Chemistry, College of Sciences, Northeastern University, Shenyang 110819, China
[3] State Key Laboratory of Electrical Insulation and Power Equipment, Center of Nanomaterials for Renewable Energy (CNRE), School of Electrical Engineering, Xi'an Jiaotong University, Xi'an 710049, China
* Correspondence: kangjing16@mails.jlu.edu.cn (J.K.); jinying.zhang@mail.xjtu.edu.cn (J.Z.); dongali@imu.edu.cn (A.D.)

How To Cite: Shen, Q.; Li, Z.; Zhao, X.; et al. Bacteria-Identifiable 2D Violet Phosphorene-Based Nanosystems for Sepsis Diagnosis and Blood Disinfection. *Advanced Antibacterial Materials* **2025**.

Received: 16 August 2025
Revised: 4 September 2025
Accepted: 5 September 2025
Published: 16 September 2025

Abstract: Despite the availability of various bacterial detection and elimination technologies, the sensitive diagnosis and treatment of sepsis caused by bloodstream infections remain significant challenges. Here, we report a magnetic nanosystem VPNS@PEI-Fe_3O_4-Apt based on functionalized two-dimensional violet phosphorus nanosheets (VPNS) by iron oxide magnetic nanoparticles (Fe_3O_4), and bacteria-specific recognition aptamers (Apt) for early sepsis diagnosis and complete in vitro blood disinfection. We demonstrated that the VPNS@PEI-Fe_3O_4-Apt nanosystem can achieve the identification and enrichment of bacterial species in blood, resulting in the successful diagnosis of sepsis caused by a single bacterium (*Staphylococcus aureus*) or multiple bacteria (*Staphylococcus aureus* and *Escherichia coli*). The strategy of VPNS@PEI-Fe_3O_4-Apt nanosystem has high detection sensitivity (~10 colony-forming units), while significantly reducing diagnostic turnaround time to within 2 h, suggesting that it has great potential for diagnosing early sepsis in clinical therapy. Furthermore, owing to the antibacterial ability derived from the excellent photodynamic (PDT) effect of VPNS and its good biocompatibility, efficient and safe complete disinfection of blood in vitro is achieved. We believe that the VPNS@PEI-Fe_3O_4-Apt magnetic nanosystem provides a new strategy for bacterial detection and treatment of sepsis.

Keywords: violet phosphorus nanosheets; specific identification; magnetic nanosystem; sepsis treatment

1. Introduction

Sepsis is a typical severe infection syndrome caused by pathogenic bacteria, which can lead to tissue damage and multi-system organ failure in severe cases, resulting in high morbidity and mortality in clinical patients [1–3]. Prompt diagnosis and treatment of sepsis enable earlier interventions, significantly improving patient outcomes and enhancing overall survival rates [4,5]. Therefore, there is an urgent need to develop high-performance strategies capable of rapidly detecting and eliminating pathogenic bacteria in the bloodstream without relying on antibiotics.

The primary methods for detecting bacteria in blood are blood culture and polymerase chain reaction (PCR) techniques. Blood culture typically involves labor-intensive and time-consuming biochemical processes, which limit its suitability for rapid detection. Meanwhile, PCR-based analysis, while offering higher sensitivity and specificity, faces challenges in practical diagnostic applications due to complex procedures and the potential for false-positive results [6–8]. Therefore, A highly accurate and rapid bacterial detection method to facilitate the early diagnosis of sepsis is an urgent need. However, the concentration of bacteria in blood is extremely low and is

confounded by the presence of various blood components, leading to significant interference from the complex matrix and subsequently making bacterial enrichment and identification particularly challenging [9–11]. In clinical practice, bacterial enrichment and subsequent identification are typically performed in separate steps, which can substantially compromise the accuracy and efficiency of the detection process. Consequently, integrating bacterial enrichment and strain identification into a single step would be an effective approach for achieving rapid and accurate diagnosis of early sepsis [12,13]. Magnetic nanoscale systems are widely employed for the enrichment of diverse targets, while aptamers exhibit superior performance in precisely recognizing target microorganisms [14–17]. Therefore, employing aptamer-functionalized magnetic nanoparticles for simultaneous bacterial enrichment and species identification represents an effective strategy for early diagnosis of sepsis.

The advent of in vitro disinfection technology has introduced a promising approach to the management of sepsis. The efficacy of sepsis treatment can be significantly enhanced by employing methods such as antibiotic treatment, heat processing, ultraviolet irradiation, and photodynamic therapy (PDT) for the disinfection of patients' blood before transfusion [16,18]. PDT exhibits significant antibacterial activity against resistant bacteria and has no adverse effects on plasma, making it a highly promising solution for in vitro blood sterilization [19]. Two-dimensional VPNS have been widely used in the biomedical field because of their excellent PDT performance and good biocompatibility, which provides a new material for the early diagnosis and treatment of sepsis. Compared with two-dimensional materials outside the phosphorus family, such as MXene or GO, VPNS has advantages such as an adjustable band gap, broad-spectrum optical effect, high carrier mobility, good biocompatibility, and biodegradability. [20–23].

Herein, we report bacterial species-identifiable magnetic nanosystems for early sepsis diagnosis and efficient in vitro blood disinfection, based on violet phosphorus nanosheets (VPNS) functionalized with iron oxide magnetic nanoparticles (Fe_3O_4) and bacterial species-identifiable aptamers (VPNS@PEI-Fe_3O_4-Apt) (Scheme 1). Aptamer modification is employed to confer bacterial capture and species identification capabilities upon the magnetic nanoparticles. The introduction of polyethyleneimine (PEI) molecules into the surface modification of VPNS enhances both the stability and biocompatibility of the magnetic system. The VPNS@PEI-Fe_3O_4-Apt system first precisely enriches bacteria, and then uses the PDT method with LED light irradiation for blood disinfection. This can effectively prevent bacterial resistance and hemolysis of blood cells, while also improving the problems of long detection time and complex procedures for bacteria in the blood. The VPNS@PEI-Fe_3O_4-Apt magnetic nanosystem provides a new strategy for bacterial detection and treatment of sepsis.

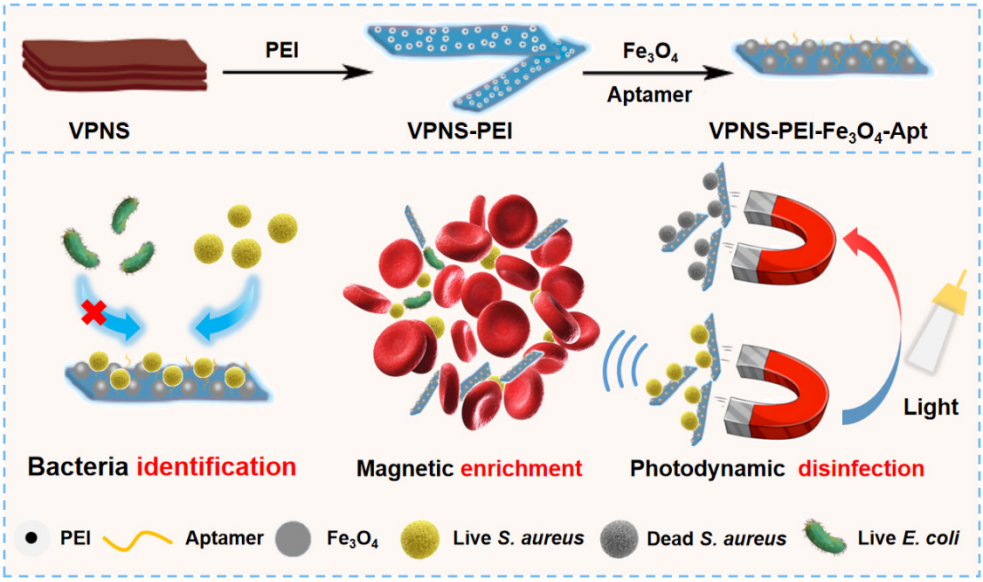

Scheme 1. Schematic illustration of the material preparation process for the VPNS@PEI-Fe_3O_4-Apt magnetic nanosystem for sepsis diagnosis and blood disinfection.

2. Materials and Methods

2.1. Materials

Violet phosphorus (VP) was supplied by the State Key Laboratory of Electrical Insulation and Power Equipment, Center of Nanomaterials for Renewable Energy, School of Electrical Engineering of Xi'an Jiaotong University (Xi'an, China). Polyethyleneimine (PEI) was purchased from Aladdin Biochemical Technology Co.,

Ltd. (Shanghai, China). Sodium chloride (NaCl), sodium hydroxide (NaOH), ethanol absolute (C_2H_6O), ammonia water ($NH_3 \cdot H_2O$), and ferric chloride ($FeCl_3$) were obtained from Tianjin Fengchuan Chemical Reagent Technologies Co., Ltd. (Tianjin, China). All chemicals were used without further purification. Microbiological culture media, including yeast extract powder and tryptone, were bought from Guangdong Huankai Biotech Co., Ltd. Beef cream was obtained from Beijing Aoboxing Biotech Co., Ltd. (Beijing, China). Agar was provided by Beijing Kulaibo Technology Co., Ltd. (Beijing, China). The microbial culture media were biological-reagent grade. Distilled water was used in all experiments and was generated by a Millipore system (Millipore Inc., Shanghai, China). The live/dead cytotoxicity kit was purchased from Keygen Biotechnology Co., Ltd. (Nanjing, China).

2.2. Preparation of Violet Phosphorene Nanosheets (VPNS)

Violet phosphorene nanosheets (VPNS) were synthesized via a convenient strategy based on a solvent exfoliation method. Typically, 80 mg of bulk VP was prepared in advance by grinding it in a mortar and then adding it to 150 mL of ethanol absolute solvent. The suspension was ultrasonicated for 30 min using an ultrasonic cleaner at 200 W. Next, the suspension was ultrasonicated at 650 W and 98% power using an ultrasonic homogenizer (JY92-IIN Ningbo Xinzhi Biotech Co., Ltd., Ningbo, China) for 2 h under an ice bath. The obtained dispersion was centrifuged at 1000 rpm for 10 min to remove the non-exfoliated bulk VP, then the supernatant was centrifuged at 15,000 rpm for 20 min to obtain ultrathin VPNS. After centrifugation, VPNS powder was obtained by triple washing with ultra-pure water and then vacuum freeze-drying.

2.3. The Synthesis of VPNS@PEI

Firstly, dissolve 15 mg of VPNS in 25 mL of deionized water, sonicate for 30 min, and then mix polyethyleneimine (PEI) with VPNS in ratios of 5:1, 10:1, and 20:1, stir overnight at room temperature at 800 rpm. After the reaction is complete, centrifuge at 10,000 rpm for 15 min, collect the precipitate, and wash it three times with deionized water. Finally, freeze dry with a freeze dryer to obtain VPNS@PEI solid powder.

2.4. Preparation of Fe_3O_4

Magnetic Fe_3O_4 is synthesized by the hydrothermal method. Dissolve 14 g $FeCl_3 \cdot 6H_2O$ and 10 g $FeSO_4 \cdot 7H_2O$ in 50 mL of deionized water and bubble with N_2 for 15 min. After adding 30 mL of ammonia, adjust the pH to about 10 with NaOH, and then stir at 75 °C for 3 h under N_2 protection to obtain magnetic Fe_3O_4 nanoparticles.

2.5. Preparation of VPNS@PEI-Fe_3O_4-Apt

Take 1.0 mg of VPNS@PEI and 2.0 mg Fe_3O_4 dissolved in deionized water and stir overnight at room temperature at a speed of 800 rpm. Then centrifuge at 10,000 rpm for 15 min, collect the precipitate, and wash it three times with deionized water. Freeze-dry it with a freeze dryer to obtain VPNS@PEI-Fe_3O_4 solid powder.

Take 1 mg of VPNS@PEI-Fe_3O_4 and 500 nM aptamer dissolved in deionized water and shake overnight. Make the aptamer-loaded VPNS@PEI-Fe_3O_4 centrifuge at 10,000 rpm for 15 min, collect the precipitate and wash it three times with deionized water, freeze dry it with a freeze dryer, and obtain VPNS@PEI-Fe_3O_4-Apt solid powder.

2.6. Bacterial Enrichment Efficiency Test of VPNS@PEI-Fe_3O_4-Apt

Prepare different concentrations of VPNS@PEI-Fe_3O_4-Apt sample, and add different concentrations of single or mixed bacterial solutions to the above suspension. Place the magnet on one side of the centrifuge tube containing the above mixture, and extract the mixture at different time points for bacterial flooring. Agar plates are cultured in a constant temperature incubator at 37 °C, and the enrichment efficiency is calculated using the following formula:

$$\text{Enrichment Efficiency\%} = 1 - (B - A)/B \times 100\% \quad (1)$$

Among them, A is the number of surviving bacteria at different time points, and B is the number of surviving original bacterial colonies.

2.7. Characterization of VPNS@PEI-Fe_3O_4-Apt

The morphology and thickness of the VPNS were observed using a Hitachi SU8010 Field Emission Scanning Electron Microscope (FESEM) (Shimadzu Co., Ltd, Kyoto, Japan) at 5.0 kV, a Tecnai G2 20 transmission electron microscope (TEM) (Japan Electronics Co., Ltd, Tokyo, Japan), and UV-vis absorption spectroscopy was performed using a Lambda 1050+ Perkin Elmer. Fluorescence spectra were tested with Hitachi Gaoxin F-4600

(PerkinElmer Instruments Co., Ltd, Shanghai, China). The zeta potential was tested with the Malvern Panaco Zetasizer Pro (Malvern Panalytical Co., Ltd, Shanghai, China).

2.8. Bacterial Cell Culture

Escherichia coli (*E. coli*, ATCC 8099, and K12, a Gram-negative bacterium) and *Staphylococcus aureus* (*S. aureus*, ATCC 6538, a Gram-positive bacterium) were used as the two model strains in antibacterial tests. Briefly, a single colony was inoculated under constant shaking at an average speed of 220 rpm in 5.0 mL of Luria-Bertani growth medium (LB) at 37 °C for 12 h, then the culture was allowed to expand to 10^8–10^9 colony forming units (CFU) mL^{-1}.

The aptamer sequence for specific recognition of *S. aureus* is:

5′- GCTAACCCCCCCAGTCCGTCCTCCCAGCCTCACACCGCCA-3′.

2.9. Antibacterial Assay

The antibacterial activity of VPNS@PEI-Fe_3O_4-Apt was evaluated by the colony-counting method using *Staphylococcus aureus* (*S. aureus*, ATCC 6538 Gram-positive bacteria). Generally, the bacterial strains were incubated in a shaker at a speed of 220 rpm for 12 h and a temperature of 37 °C to obtain bacterial strain concentrations of 10^8–10^9 CFU·mL^{-1} for subsequent use. First, 1 mL of bacterial liquid with a concentration of 10^8–10^9 CFU·mL^{-1} was absorbed and centrifuged at a speed of 4000 rpm for 7 min. Next, the liquid medium was poured out, and the precipitated bacterial strains were washed three times with 0.8 wt% sodium chloride aqueous solution and then redispersed in 1 mL of sterile distilled water. The bacteria concentration was diluted to 10^7 CFU·mL^{-1}. 1.0 mg of VPNS@PEI-Fe_3O_4-Apt was dispersed in 900 μL of sterile distilled water, and 100 μL of the above bacterial liquid was added, and then put into a shaker for 2 h at room temperature. The mixture was diluted step by step to 10^2 CFU·mL^{-1} and spread evenly on LB agar plates. The mixture was inverted in an incubator at 37 °C for 24 h under LED white light. All experiments were repeated three times, and the antibacterial rate was calculated according to the following formula:

$$\text{Antibacterial Rate\%} = (B - A)/B \times 100\% \quad (2)$$

where A is the number of surviving colonies for the sample and B is the number of surviving colonies for the control.

2.10. CCK-8 Assay

The cytotoxicity was evaluated by CCK-8 in vitro cytotoxicity analysis with NIH 3T3 as the cell model. Specifically, NIH 3T3 cells (7000 cells/well) were inoculated in a 96-well plate containing 180 μL and incubated at 37 °C for 24 h. The VPNS@PEI-Fe_3O_4-Apt were dispersed with sterile PBS, and the samples were prepared at concentrations of 0.125, 0.25, 0.5, and 1.0 mg·mL^{-1}. Next, 20 μL of the VPNS@PEI-Fe_3O_4-Apt was added to each well of NIH 3T3 cells cultured as described above, then incubated at 37 °C for 24 h. The cultured mixture was washed twice with PBS, and into each well was added 150 μL of the prepared 10% (*v*/*v*) CCK-8 solution, and the wells were incubated at 37 °C for 2 h. The OD value at 450 nm was measured with a microplate microscope.

2.11. Hemolysis Test

Fresh blood was harvested from BALB/c mice, then it was centrifuged at 1500 rpm for 10 min in 1 × PBS (pH = 7.2) to remove broken red blood cells. An erythrocyte suspension was incubated with VPNS samples in different concentrations (2.0–0.0625 mg·mL^{-1}) at 37 °C for 2 h. Triton X-100 was used as the positive control, while PBS buffer was used as the negative control. After incubation, the VPNS@PEI-Fe_3O_4-Apt sample was removed, and the erythrocyte stock solution was centrifuged at 1500 rpm for 10 min to obtain the supernatant. Then the absorbance of the supernatant was measured at 578 nm using the UV-vis spectrum (HITACHI U3900). The hemolysis rate was calculated by the following formula:

$$\text{Hemolysis (\%)} = (A - A_{PBS}/A_0 - A_{PBS}) \times 100\% \quad (3)$$

where A is the absorbance of the VPNS, A_0 is the absorbance of the positive control Triton X-100, and A_{PBS} is the absorbance of the negative control PBS buffer.

2.12. Disinfection Experiment of VPNS@PEI-Fe_3O_4-Apt

The mice were obtained from the Animal Center of Inner Mongolia University, and all animal experiments were approved by the university's Institutional Review Board (IMU-2023/037). Animal husbandry was performed

following the Ministry of Health of the People's Republic of China's Guidelines on Animal Management and the Chinese Guide for the Use of Laboratory Animals in Husbandry. Using a mouse blood disinfection experiment to evaluate VPNS@PEI-Fe_3O_4-Apt disinfection of bacteria in the blood. This study introduced 100 CFU of *S. aureus* bacteria into the blood circulation system of mice through the tail vein pathway to establish a blood-infected mouse model. Collect sepsis blood samples from the orbital venous plexus of infected mice 1 h later. Add the collected blood sample to a solution with a concentration of 1.0 mg·mL^{-1} VPNS@PEI-Fe_3O_4-Apt and perform magnetic enrichment treatment on the sample for 120 min. Finally, the blood biochemical index was tested on the processed blood.

3. Results and Discussion

As illustrated in Figure 1a, scanning electron microscopy (SEM) showed bulk violet phosphorus (VP) to have a multilayer structure. The violet phosphorene nanosheets (VPNS), featuring a thin-layer two-dimensional morphology, were obtained via a solvent exfoliation method from bulk VP under mild conditions. The TEM image shows that the VPNS have a wide range of two-dimensional sizes and a large surface area, which makes them great candidates for loading materials (Figure 1b). The charge modification was carried out by coating PEI on the surface of VPNS with a strong electrostatic interaction. STEM mapping analysis showed the presence and uniform distribution of elemental phosphorus in all samples, further indicating the high purity of VPNS (Figure 1c). As shown in Figure 1d, the surface of VPNS is rich in negative charge, which is converted to positive charge by the coating charge of PEI in different proportions. With the increase in the coating ratio, the positive charge gradually increases. When the ratio of VPNS and PEI increases to 1:20, the potential increases to +35.2 eV, indicating the successful coating of PEI on the VPNS surface. Fourier transform infrared spectroscopy (FT-IR) further reveals the successful preparation of VPNS@PEI. As shown in Figure 1e, the characteristic absorption peaks at 2971 cm^{-1} and 2842 cm^{-1} can be attributed to the stretching vibration of C–H bonds, while the absorption peak at 1571 cm^{-1} corresponds to the bending vibration of N–H bonds.

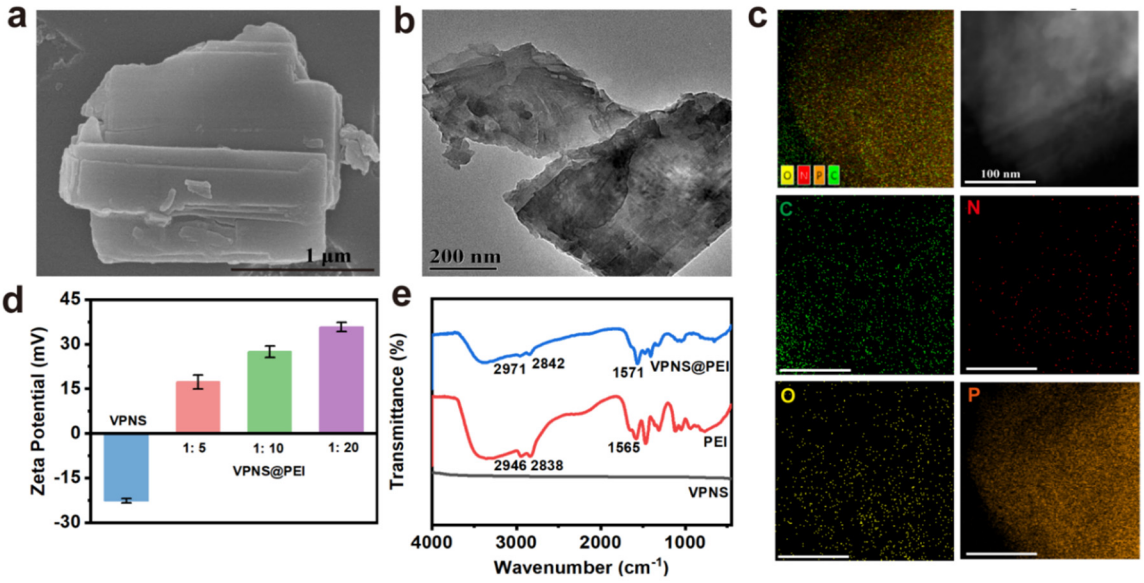

Figure 1. (**a**) SEM image of bulk VP. (**b**) TEM image of VPNS. (**c**) Representative STEM mapping of VPNS. (**d**) Zeta potential of VPNS@PEI at different proportions. (**e**) FTIR spectra of VPNS@PEI.

Magnetic Fe_3O_4 was synthesized by a simple hydrothermal synthesis process; the average particle size was about 10 nm (Figure 2a). Magnetic Fe_3O_4 nanoparticles and aptamers that can specifically recognize *S. aureus* were loaded onto the surface of VPNS@PEI via electrostatic interactions, endowing the nanosystem with enhanced magnetic recovery capabilities and specific bacterial recognition properties. The TEM image shows that the Fe_3O_4 nanoparticles were evenly distributed on the surface of VPNS@PEI (Figure 2b,c). Figure 2d,e shows the changes in potential and the results of magnetic absorption recovery experiments during the synthesis process, which further confirm the successful synthesis of VPNS@PEI-Fe_3O_4-Apt. In addition, the successful preparation of the VPNS@PEI-Fe_3O_4-Apt was further characterized by the decrease in the characteristic absorption peak of the aptamer at 260 nm as determined by ultraviolet–visible (UV-Vis) spectroscopy of the supernatant (Figure 2f).

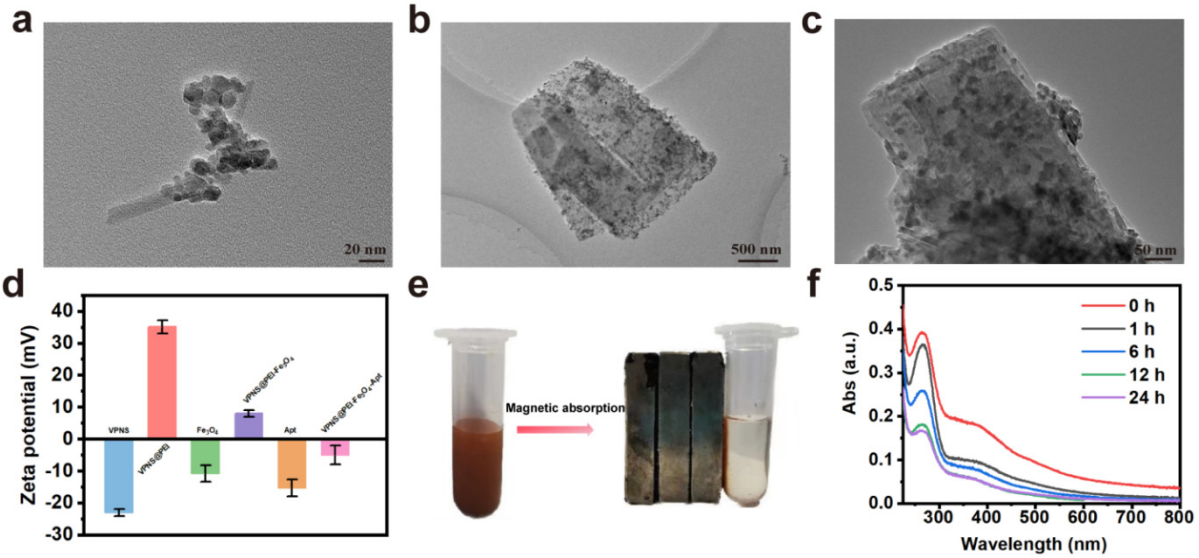

Figure 2. (**a**) TEM image of Fe_3O_4. (**b**,**c**) TEM image of VPNS@PEI-Fe_3O_4. (**d**) Zeta potential changes during the synthesis process VPNS@PEI-Fe_3O_4-Apt. (**e**) Digital photo of VPNS@PEI-Fe_3O_4-Apt under applied magnetic field. (**f**) UV-Vis spectra of the loaded Apt supernatant.

To evaluate the bacterial identification and enrichment performance of the VPNS@PEI-Fe_3O_4-Apt nanosystem, bacterial separation and magnetic enrichment experiments were conducted after co-incubating the VPNS@PEI-Fe_3O_4-Apt nanosystem with pathogenic bacteria *S. aureus.* As shown in Figure 3a, the VPNS@PEI-Fe_3O_4-Apt nanosystem exhibits a bacterial separation effect related to incubation time and achieves almost complete bacterial enrichment in a short period of time (about 120 min). Surprisingly, the presence of aptamers increased the enrichment efficiency of bacteria. Following the completion of bacterial enrichment, the unenriched bacterial solution was quantified via plate counting. Notably, a substantial number of bacteria remained viable on the plates for the VPNS@PEI-Fe_3O_4 group, whereas only a limited number of colonies were observed on the plates for the VPNS@PEI-Fe_3O_4-Apt group, indicating that the aptamer significantly contributed to the efficiency of bacterial capture (Figure 3a insert). The ability of different concentrations of VPNS@PEI-Fe_3O_4-Apt to capture bacteria was further explored. As shown in Figure 3b, more than 99.9% of bacteria can be captured when the sample concentration is 1.0 $mg \cdot mL^{-1}$, and the capturing ability of bacteria only decreases slightly with the decrease in sample concentration. To ensure the safe in vivo application of VPNS@PEI-Fe_3O_4-Apt, the concentration efficiency of *S. aureus* was evaluated in water, PBS, and blood environments. As shown in Figure 3c, high enrichment efficiency is still maintained in different solution environments, indicating that the material has environmental stability. To further validate the specific binding capability of aptamers to *S. aureus*, we evaluated the enrichment efficiency of VPNS@PEI-Fe_3O_4-Apt across various bacterial strains. As illustrated in Figure 3d, VPNS@PEI-Fe_3O_4-Apt demonstrated a high enrichment efficiency exceeding 90% for *S. aureus*, confirming its high specificity. In contrast, the enrichment efficiency for *E. coli*, which is non-specifically recognized, was less than 40%. Subsequently, VPNS@PEI-Fe_3O_4-Apt was incubated with a mixed bacterial suspension to further evaluate its specific recognition capability. As illustrated in Figure 3e, VPNS@PEI-Fe_3O_4-Apt demonstrated the ability to enrich over 95.4% of *S. aureus* from the mixed bacterial suspension. In contrast, the enrichment efficiency for *E. coli* was only 28.7%, indicating that the sample exhibits high specificity towards *S. aureus* and effectively enriches the target bacteria. It is worth noting that the bacterial concentration used in the above tests was relatively high (approximately 10^6 colony-forming units (CFU)). To evaluate the performance of the VPNS@PEI-Fe_3O_4-Apt nanosystem, it is necessary to conduct bacterial enrichment at low concentrations. As illustrated in Figure 3f, the VPNS@PEI-Fe_3O_4-Apt nanosystem exhibits a high bacterial enrichment capacity of approximately 90% for low bacterial concentrations ranging from 10^6 to 10 CFU. Notably, the system successfully identified and enriched bacteria even at extremely low concentrations (10 CFU), which provided the extremely high sensitivity of the nanosystem.

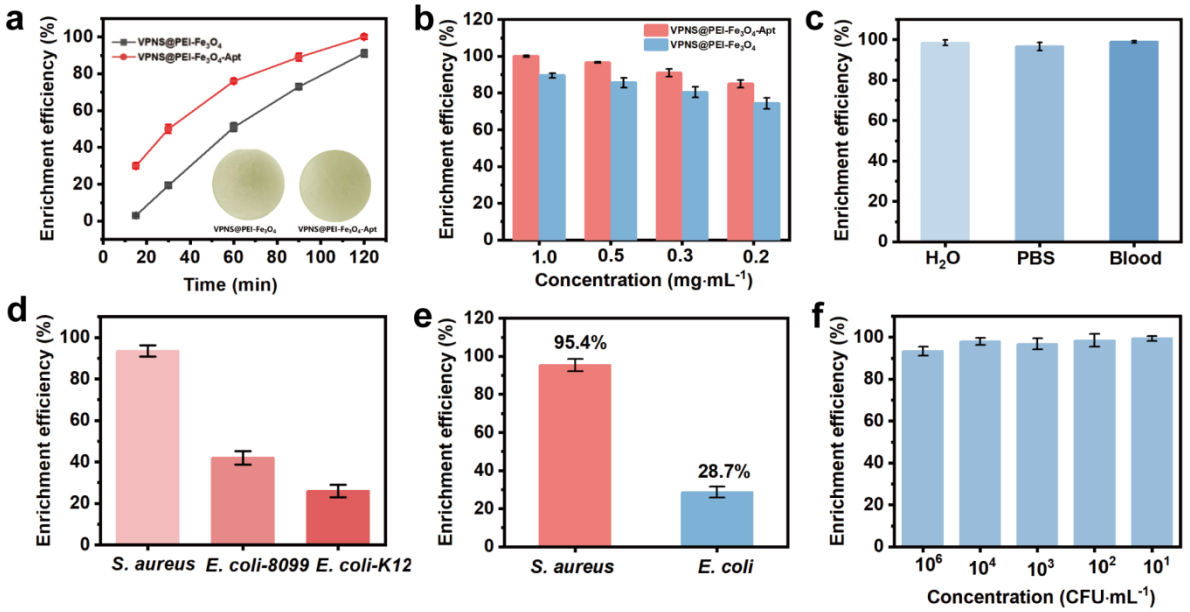

Figure 3. (**a**) Enrichment efficiency of VPNS@PEI-Fe_3O_4-Apt for *S. aureus,* insert: enrichment plate images of VPNS@PEI-Fe_3O_4-Apt for *S. aureus*. (**b**) Enrichment efficiency of *S. aureus* at different concentrations of VPNS@PEI-Fe_3O_4-Apt. (**c**) Enrichment efficiency of VPNS@PEI-Fe_3O_4-Apt against *S. aureus* in different solution environments. (**d**) VPNS@PEI-Fe_3O_4-Apt enrichment efficiency of different bacterial strains. (**e**) VPNS@PEI-Fe_3O_4-Apt enrichment efficiency of mixed bacteria. (**f**) Enrichment efficiency of VPNS@PEI-Fe_3O_4-Apt to different concentrations of bacteria.

The efficiency of killing the enriched bacteria serves as a critical indicator for evaluating the therapeutic efficacy of sepsis treatment (Figure 4a). Using the colony-counting method, we evaluated the antibacterial action of VPNS@PEI-Fe_3O_4-Apt against 10^7 CFU·mL^{-1} of *S. aureus*, after exposure to 1.0 mg·mL^{-1} of VPNS@PEI-Fe_3O_4-Apt for 2 h under LED white light irradiation, the antibacterial percentage of VPNS@PEI-Fe_3O_4-Apt reached >99% (Figure 4b). The antibacterial rate of around 25% at a concentration as low as 0.05 mg·mL^{-1}, indicating that VPNS@PEI-Fe_3O_4-Apt has excellent antibacterial performance. VPNS@PEI-Fe_3O_4-Apt can effectively kill the bacteria accumulated and has a concentration-dependent property. VPNS can produce four ROS signals under light irradiation: singlet oxygen ($^1O_2$), superoxide anion radical ($\cdot O_2^-$), hydrogen peroxide (H_2O_2), and hydroxyl radical (·OH), respectively [22]. The PDT effect of VPNS@PEI-Fe_3O_4-Apt was evaluated with a typical ROS probe, 2,7-DCFH-DA (2′,7′-Dichlorodihydrofluorescein diacetate), which can be converted into fluorescent 2-(3,6-Diacetoxy-2,7-dichloro-9H-xanthen-9-yl) benzoic acid (DCF) in the presence of ROS. In the co-incubation of VPNS@PEI-Fe_3O_4-Apt with DCFH-DA under LED irradiation for 120 min, the oxidized DCF exhibited a strong fluorescence peak around 525 nm. As illustrated in Figure 4c, the characteristic absorption peaks intensify progressively with prolonged light exposure, indicating significant reactive oxygen species (ROS) generation. In conclusion, the VPNS@PEI-Fe_3O_4-Apt nanocomposite demonstrates significant antibacterial efficacy by ROS via PDT effect.

In addition to enrichment capacity and antibacterial activity, it is essential to evaluate the biocompatibility of VPNS@PEI-Fe_3O_4-Apt before applying it *in vivo*. First, the cell cytotoxicity of VPNS was assessed using CCK-8 assays (Figure 4d). The VPNS@PEI-Fe_3O_4-Apt showed no toxicity toward NIH 3T3 cells within a concentration range of 0.125–2.0 mg·mL^{-1}, suggesting VPNS have good biocompatibility and hence potential for use in clinical applications. Figure S1 showed that there was no significant difference between cell viability exposed to LED light for 180 min and cell viability exposed to LED light for 0 min, indicating that long-term light had no effect on cell viability. In addition, we also performed hemolysis testing to further evaluate the erythrocyte compatibility of VPNS, using Triton X-100 as the positive control. As shown in Figure 4e, after incubation with the VPNS@PEI-Fe_3O_4-Apt, followed by centrifugation, the supernatants were transparent, indicating that no disruption of the erythrocytes occurred and no hemoglobin was released. The hemolysis rate of the VPNS@PEI-Fe_3O_4-Apt was only 3.2% at 2.0 mg·mL^{-1}, much lower than the ASTM standard (ASTM F756-2008) for the hemolysis ratio of biomaterials (<5%).

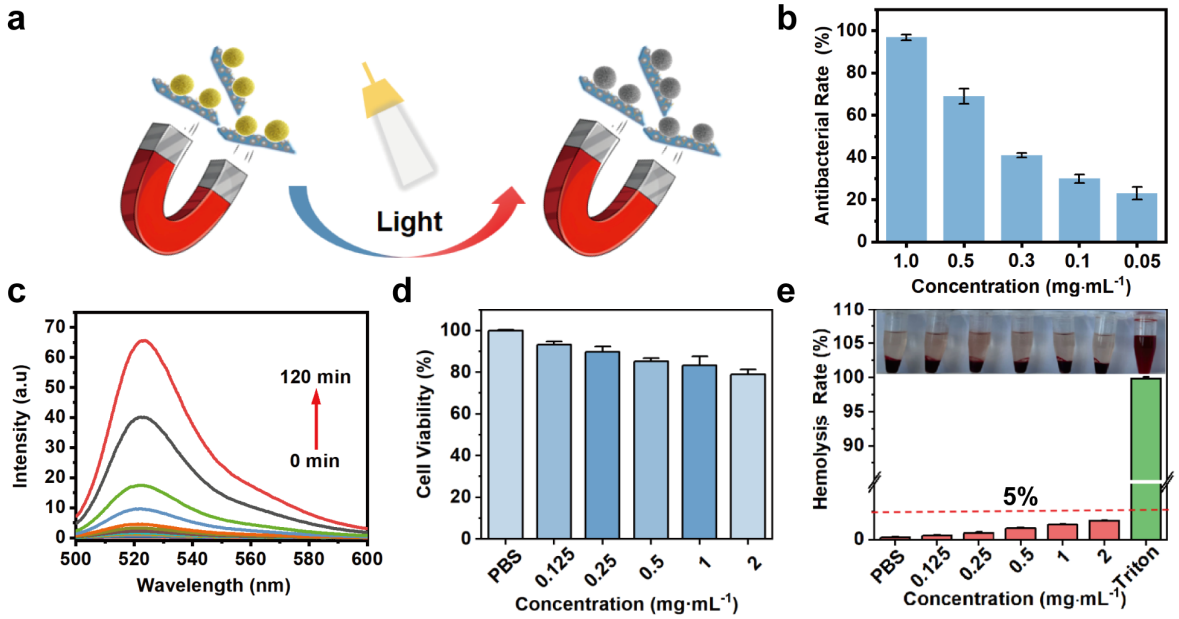

Figure 4. (**a**) Schematic diagram of VPNS@PEI-Fe_3O_4-Apt killing bacteria under light conditions. (**b**) Antibacterial rate of different concentrations of VPNS@PEI-Fe_3O_4-Apt. (**c**) Fluorescence absorption spectrum of DCFH-DA solution with VPNS@PEI-Fe_3O_4-Apt under LED light irradiation. (**d**) Cytotoxicity of VPNS@PEI-Fe_3O_4-Apt within the concentration range 0.125–2.0 mg·mL^{-1}. (**e**) Hemolysis rate of VPNS@PEI-Fe_3O_4-Apt, and corresponding digital photos.

To construct a mouse model of blood infection, 100 CFU of S. aureus was injected into the tail vein of mice. Sepsis blood samples were subsequently collected from the orbital venous cluster of infected mice (Figure 5a). The impact of VPNS@PEI-Fe_3O_4-Apt on blood disinfection was assessed through the evaluation of biochemical indicators in blood samples. Blood of healthy mice and blood infected with bacteria were used as the negative control and positive control, respectively. The levels of white blood cells (WBC), platelets (PLT), red blood cells (RBC), and neutrophils (Gran) were tested to evaluate the hematological health status. As shown in Figure 5b–e, in the positive control group, the levels of WBC and Gran were significantly elevated, indicating the presence of inflammation and infection. Conversely, following VPNS@PEI-Fe_3O_4-Apt treatment, the WBC and Gran levels were restored to within the normal reference range, suggesting that the inflammatory response had been effectively suppressed. PLT is an important indicator for evaluating blood clotting function, which is crucial for stopping bleeding and wound healing. RBC can be used to reflect whether there is anemia or other blood diseases. The PLT and RBC indicators in the sample treatment group are all within the normal range, indicating normal blood coagulation function and no blood diseases were found. In addition, Whole blood from mice was collected for comprehensive biochemical analysis, as illustrated in Figure 5f–k. The evaluated parameters included albumin (ALB), creatinine (CREA), creatine kinase (CK), alkaline phosphatase (ALP), urea (UREA), and lactate dehydrogenase (LDH). The results showed that there was no significant difference in biochemical indexes between the experimental group and the control group, indicating that the blood treated by VPNS@PEI-Fe_3O_4-Apt had recovered to a healthy level and had no influence on physiological function. Based on these results, we believe that the VPNS@PEI-Fe_3O_4-Apt nanosystem can safely and effectively treat blood infections in vitro, laying a foundation for the development of automated in vitro blood disinfection systems for clinical sepsis treatment.

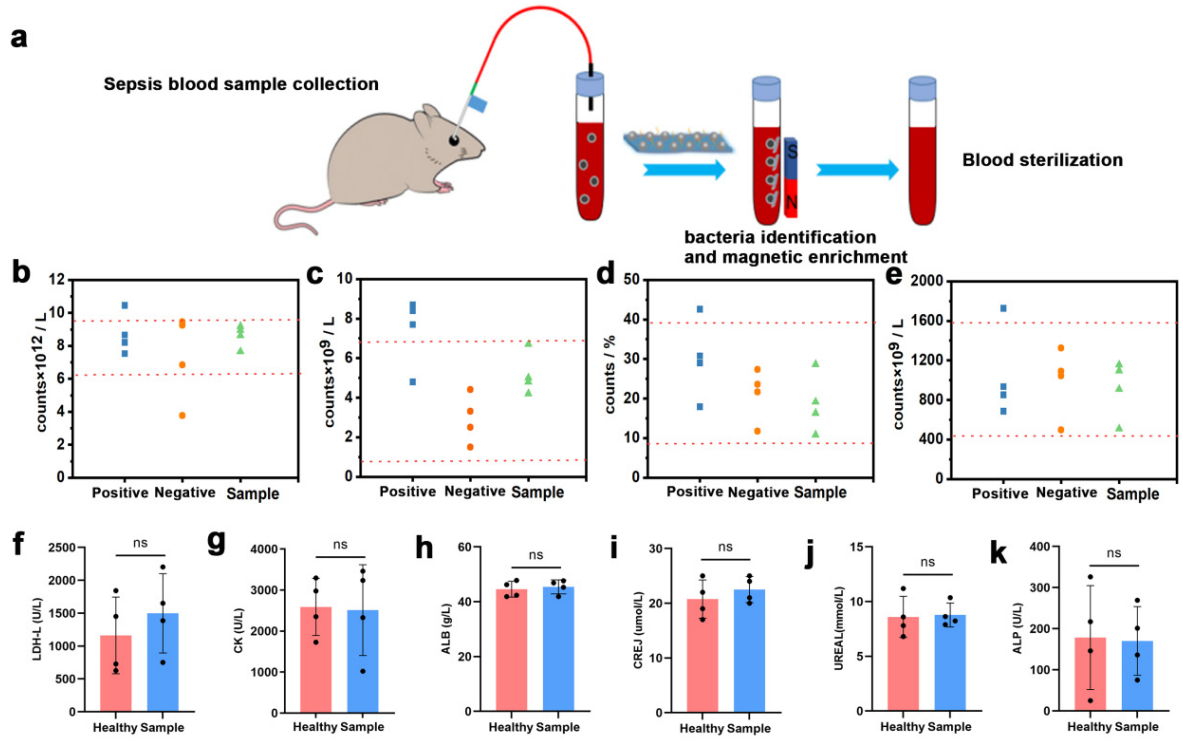

Figure 5. (**a**) Schematic diagram of VPNS@PEI-Fe_3O_4-Apt used for blood sterilization. Analysis of (**b**) WBC, (**c**) RBC, (**d**) Gran, and (**e**) PLT index of blood treated with VPNS@PEI-Fe_3O_4-Apt. Analysis of (**f**) LDH-L, (**g**) CK, (**h**) ALB, (**i**) CREJ, (**j**) UREREAL, and (**k**) ALP indicators of blood treated with VPNS@PEI-Fe_3O_4-Apt.

4. Conclusions

In summary, we report bacterial species-identifiable magnetic nanosystems for early sepsis diagnosis and efficient extracorporeal blood disinfection. We demonstrated that the VPNS@PEI-Fe_3O_4-Apt nanosystem can achieve identification and enrichment of bacterial species in blood in one step. The enrichment efficiency of *S. aureus* was up to 90% for both single and mixed bacteria. Moreover, the VPNS@PEI-Fe_3O_4-Apt nanosystem strategy demonstrated high detection sensitivity, capable of identifying approximately 10 colony-forming units (CFUs), while significantly reducing the diagnostic turnaround time to within 2 h The results indicate its substantial potential for early sepsis diagnosis in clinical settings. In addition, owing to the excellent PDT effect of VPNS and their superior biocompatibility, efficient and safe complete blood disinfection was achieved in vitro. We believe that the VPNS@PEI-Fe_3O_4-Apt magnetic nanosystem provides a new strategy for bacterial detection and treatment of sepsis.

Supplementary Materials

The additional data and information can be downloaded at: https://media.sciltp.com/articles/others/25091609 41253520/AAM-2508000294-SI-FC.pdf. Figure S1: The cell viability of cells under LED white light for 0 min and 120 min.

Author Contributions

Q.S., J.K. and A.D. designed the research plan. Q.S. and X.Z performed the experiments and analyzed the data. Q.S., Z.L. and A.D. worked on the figures. Q.S. contributed to the writing of the manuscript. J.K. and A.D. refined the draft. J.Z. provided technical support and conceptual advice. All authors discussed the results and implications and edited the manuscript at all stages.

Funding

This research was funded by [National Natural Science Foundation of China, Grant Number 22062017], [Natural Science Foundation of Inner Mongolia Autonomous Region, Grant Numbers 2023QN02011 and 2024ZD10], [University-Industry Collaborative Education Program, Grant Number 230904807140344], and [Research Program of Science and Technology at Universities of Inner Mongolia Autonomous Region, Grant Number NJZZ23091].

Institutional Review Board Statement

The study was conducted according to the guidelines of the Declaration of Helsinki, and approved by the Institutional Review Board (or Ethics Committee) of Animal Center of Inner Mongolia University (protocol code IMU-2023/037).

Informed Consent Statement

Not applicable.

Data Availability Statement

The data that support the findings of this study are available from the corresponding author upon reasonable request.

Conflicts of Interest

The authors have no conflicts to disclose.

References

1. Cohen, J. The immunopathogenesis of sepsis. *Nature* **2002**, *420*, 885–891.
2. Burnouf, T.; Radosevich, M. Reducing the risk of infection from plasma products: Specific preventative strategies. *Blood Rev.* **2000**, *14*, 94–110.
3. Savelkoel, J.; Claushuis, T.A.M.; van Engelen, T.S.R.; et al. Global impact of world sepsis day on digital awareness of sepsis: An evaluation using google trends. *Crit. Care* **2018**, *22*, 61.
4. Prescott, H.C.; Angus, D.C. Enhancing recovery from sepsis: A review. *JAMA* **2018**, *319*, 62–75.
5. Zampieri, F.G.; Bagshaw, S.M.; Semler, M.W. Fluid therapy for critically ill adults with sepsis: A review. *JAMA* **2023**, *329*, 1967–1980.
6. Mancini, N.; Carletti, S.; Ghidoli, N.; et al. The era of molecular and other non-culture-based methods in diagnosis of sepsis. *Clin. Microbiol. Rev.* **2010**, *23*, 235–251.
7. Meyer, T.; Franke, G.; Polywka, S.K.A.; et al. Improved detection of bacterial central nervous system infections by use of a broad-range pcr assay. *J. Clin. Microbiol.* **2014**, *52*, 1751–1753.
8. Hsieh, K.; Ferguson, B.S.; Eisenstein, M.; et al. Integrated electrochemical microsystems for genetic detection of pathogens at the point of care. *Acc. Chem. Res.* **2015**, *48*, 911–920.
9. Sunbul, M.; Jäschke, A. Contact-mediated quenching for RNA imaging in bacteria with a fluorophore-binding aptamer. *Angew. Chem. Int. Ed.* **2013**, *52*, 13401–13404.
10. Zhang, L.; Dong, W.F.; Sun, H.B. Multifunctional superparamagnetic iron oxide nanoparticles: Design, synthesis and biomedical photonic applications. *Nanoscale* **2013**, *5*, 7664–7684.
11. Gu, H.; Ho, P.L.; Tsang, K.W.T.; et al. Using biofunctional magnetic nanoparticles to capture vancomycin-resistant enterococci and other gram-positive bacteria at ultralow concentration. *J. Am. Chem. Soc.* **2003**, *125*, 15702–15703.
12. Chen, J.; Duncan, B.; Wang, Z.; et al. Bacteriophage-based nanoprobes for rapid bacteria separation. *Nanoscale* **2015**, *7*, 16230–16236.
13. Ray, P.C.; Khan, S.A.; Singh, A.K.; et al. Nanomaterials for targeted detection and photothermal killing of bacteria. *Chem. Soc. Rev.* **2012**, *41*, 3193–3209.
14. Zhou, R.; Wu, X.; Xue, S.; et al. Magnetic metal-organic frameworks-based ratiometric sers aptasensor for sensitive detection of patulin in apples. *Food Chem.* **2025**, *466*, 142200.
15. Kavruk, M.; Babaie, Z.; Kibar, G.; et al. Aptamer decorated PDA@magnetic silica microparticles for bacteria purification. *Microchim. Acta* **2024**, *191*, 285.
16. Didar, T.F.; Cartwright, M.J.; Rottman, M.; et al. Improved treatment of systemic blood infections using antibiotics with extracorporeal opsonin hemoadsorption. *Biomaterials* **2015**, *67*, 382–392.
17. Wu, L.; Wang, Y.; Xu, X.; et al. Aptamer-based detection of circulating targets for precision medicine. *Chem. Rev.* **2021**, *121*, 12035–12105.
18. Li, Z.; Luo, B.; Chen, Y.; et al. Nanomaterial-based encapsulation of biochemicals for targeted sepsis therapy. *Mater. Today Bio* **2025**, *33*, 102054.
19. Li, S.; Cui, S.; Yin, D.; et al. Dual antibacterial activities of a chitosan-modified upconversion photodynamic therapy system against drug-resistant bacteria in deep tissue. *Nanoscale* **2017**, *9*, 3912–3924.
20. Zhang, L.; Huang, H.; Zhang, B.; et al. Structure and properties of violet phosphorus and its phosphorene exfoliation. *Angew. Chem. Int. Ed.* **2020**, *59*, 1074–1080.
21. Zhao, C.; Han, X.; Wang, S.; et al. Violet phosphorus nanosheet: A biocompatible and stable platform for stimuli-responsive multimodal cancer phototherapy. *Adv. Healthc. Mater.* **2023**, *12*, 2201995.

22. Li, C.; Wu, Y.; Chen, Y.; et al. Violet phosphorene nanosheets coupled with CRISPR/Cas12a in a biosensor with a low background signal for onsite detection of tigecycline-resistant hypervirulent *Klebsiella pneumoniae*. *Sens. Actuators B: Chem.* **2023**, *395*, 134509.
23. Shen, Q.; Kang, J.; Zhao, X.; et al. Bacterial elimination via cell membrane penetration by violet phosphorene peripheral sub-nanoneedles combined with oxidative stress. *Chem. Sci.* **2024**, *15*, 4926–4937.